A&A manuscript no.
(will be inserted by hand later)

Your thesaurus codes are:
07(08.16.4;08.22.3;08.13.2;08.03.4;08.03.1;02.08.1)

ASTRONOMY
AND
ASTROPHYSICS
16.8.1996

Dust formation in winds of long-period variables

IV. Atmospheric dynamics and mass loss

S. Höfner and E.A. Dorfi

Institut für Astronomie der Universität Wien, Türkenschanzstraße 17, A-1180 Wien, Austria

Received Date; accepted date

Abstract. We have calculated radiation-hydrodynamical models of the atmosphere and circumstellar dust shell of C-rich long-period variables which include a detailed description of the dust formation process. We discuss the time-dependent behaviour of the circumstellar envelope (e.g. multiperiodicity) and its relevance for observational properties like near-IR light curves and investigate the time-averaged mass loss characteristics of a sample of models satisfying radius–luminosity–mass and period–luminosity relations. The results can be summarized as follows: The dependence of the mass loss rate on stellar parameters predicts a strong increase of mass loss as stars evolve along the AGB. The models presented agree reasonably well with mean mass loss–period relations deduced from observations of Mira stars and the observed scatter of mass loss rates for a given period can be understood in terms of pulsation amplitude or non-linearities of the wind mechanism. The wind velocities show a good correlation with the quantity $(\rho_d/\rho_g)\, L_\star/M_\star$ which characterizes the strength of radiation pressure on dust relative to gravitation.

Key words: stars: AGB and post-AGB – stars: variables – stars: mass-loss – stars: circumstellar matter – stars: carbon – hydrodynamics

1. Introduction

The investigation of mass loss on the AGB is essential for understanding the late stages of stellar evolution of low and intermediate mass stars. A large number of detailed observational and theoretical programs have been devoted to this subject during the last few years (see e.g. Habing 1996 for a recent review). From these studies it has become clear that the interaction of pulsation and dust formation plays a key role for the mass loss phenomenon. Strong shock waves caused by the stellar pulsation lead to a levitation of the stellar atmosphere, providing a cool and dense environment as required for an efficient formation and growth of dust grains. The newly formed dust grains are accelerated by the stellar radiation field and initiate a slow massive outflow by transfering momentum to the surrounding gas.

Models of increasing complexity have been constructed to investigate this process in detail. Wood (1979) and Bowen (1988) have studied the mass loss of dynamical models introducing a parameterized opacity to describe the effects of dust formation in the circumstellar envelope. Bowen & Willson (1991) discuss the implications of their models for the mass loss during AGB evolution (“superwind”). Recently, Blöcker (1995) has used a modified version of Reimers’ law based on the models of Bowen (1988) to describe mass loss in his calculations of stellar evolution on the AGB. The dynamical models of Fleischer et al. (1992) include a time-dependent description of dust formation and reveal complex phenomena like a discrete spatial structure of the circumstellar dust shell and multiperiodicity. Radiative transfer calculations by Winters et al. (1994, 1995) based on these models predict that these features will affect observable properties like brightness profiles or near-IR lightcurves. Observations seem to confirm these phenomena (e.g. Le Bertre 1992).

In the preceeding paper of this series (Höfner et al. 1995) we have presented for the first time dynamical models of the circumstellar envelope obtained by solving radiation hydrodynamics together with a detailed time-dependent description of the dust component. We have investigated the limiting case of purely dust driven winds and the dust-induced κ-mechanism (cf. Fleischer et al. 1995). In the present paper we include the effects of stellar pulsation in our calculations by applying a piston and a variable luminosity at the inner boundary (Sect. 2).

In contrast to other papers on comparable models (e.g. Fleischer et al. 1992, Winters et al. 1994, 1995, Höfner et al. 1996) which highlight certain physical (or numerical) aspects of the problem with relatively few examples we want to present a systematic investigation of how the resulting properties depend on various physical parameters of the models. In particular we concentrate on two aspects: (i) the time-dependent behaviour (periodicity) which – in combination with detailed

Send offprint requests to: S. Höfner,
Internet: hoefner@astro.ast.univie.ac.at

observations – could in principle help to constrain physical parameters of individual stars (Sect. 3) and (ii) time-averaged mass loss characteristics of a sample of models which satisfy a radius–luminosity–mass relation and a period–luminosity relation (Sect. 4). We compare our results to mean mass loss–period relations for Mira variables and discuss the implications of our models for stellar evolution on the AGB.

2. Modelling method and parameters

We solve the coupled system of radiation hydrodynamics and time-dependent dust formation (cf. Höfner et al. 1995) employing an implicit numerical method and an adaptive grid (for details of the numerical technique see Dorfi & Feuchtinger 1995). The gas dynamics including self-gravity is described by the equations of continuity, motion and energy, and the radiation field by the grey moment equations of the radiative transfer equation. The energy exchange between matter and radiation adopts a LTE source function which could result in overestimating the cooling rates behind radiative shocks. Considering C-rich stars we assume the formation of amorphous carbon grains. The extinction efficiency of the grains ($Q'_{\rm ext} = Q_{\rm ext}/a = 4.4\,T$; a: grain radius, T: temperature) is based on the optical constants of Maron (1990).

The pulsation of the long-period variable (LPV) is simulated by a sinusoidal motion of the inner boundary $R_{\rm in}$ which is located below the stellar photosphere ($R_{\rm in} = 0.91\,R_\star$). Since the radiative flux is kept constant at this point the luminosity at the inner boundary varies according to $L_{\rm in}(t) \propto R_{\rm in}(t)^2$.

The models are characterized by the following set of parameters: stellar mass $M_\star$, luminosity $L_\star$, effective temperature $T_\star$ and the carbon-to-oxygen abundance ratio $\varepsilon_{\rm C}/\varepsilon_{\rm O}$ (all abundances except carbon are assumed as solar) of the hydrostatic initial model as well as the piston parameters period P and velocity amplitude $\Delta u_{\rm p}$. For the models presented in this paper (except series P) we have calculated $T_\star$ from $M_\star$ and $L_\star$ using the radius–luminosity–mass relation of Iben (1984) with $(l/H_p) = 0.90$ and $Z = 0.020$ as in Bowen & Willson (1991) together with $\sigma T_\star^4 = L_\star/(4\pi R_\star^2)$ and have chosen P according to a period–luminosity relation for Miras (Feast et al. 1989). The physical parameters are selected to demonstrate the effects of time-dependent dust formation in LPV atmospheres which leads to a sample biased towards relatively high $\varepsilon_{\rm C}/\varepsilon_{\rm O}$ values. In this context we want to emphasize that the conclusions drawn from our calculations of C-rich objects may not be directly applicable to the large group of O-rich AGB stars.

3. Dynamics and periodicity

In general, models which include a time-dependent description of the dust component do not show a periodic temporal behaviour of the circumstellar envelope in response to a periodic driving at the inner boundary. This is due to the facts that (i) the formation and growth of dust grains is governed by its own time-scales which need not be associated with those of the pulsation (piston) and (ii) that – due to its high opacity – the

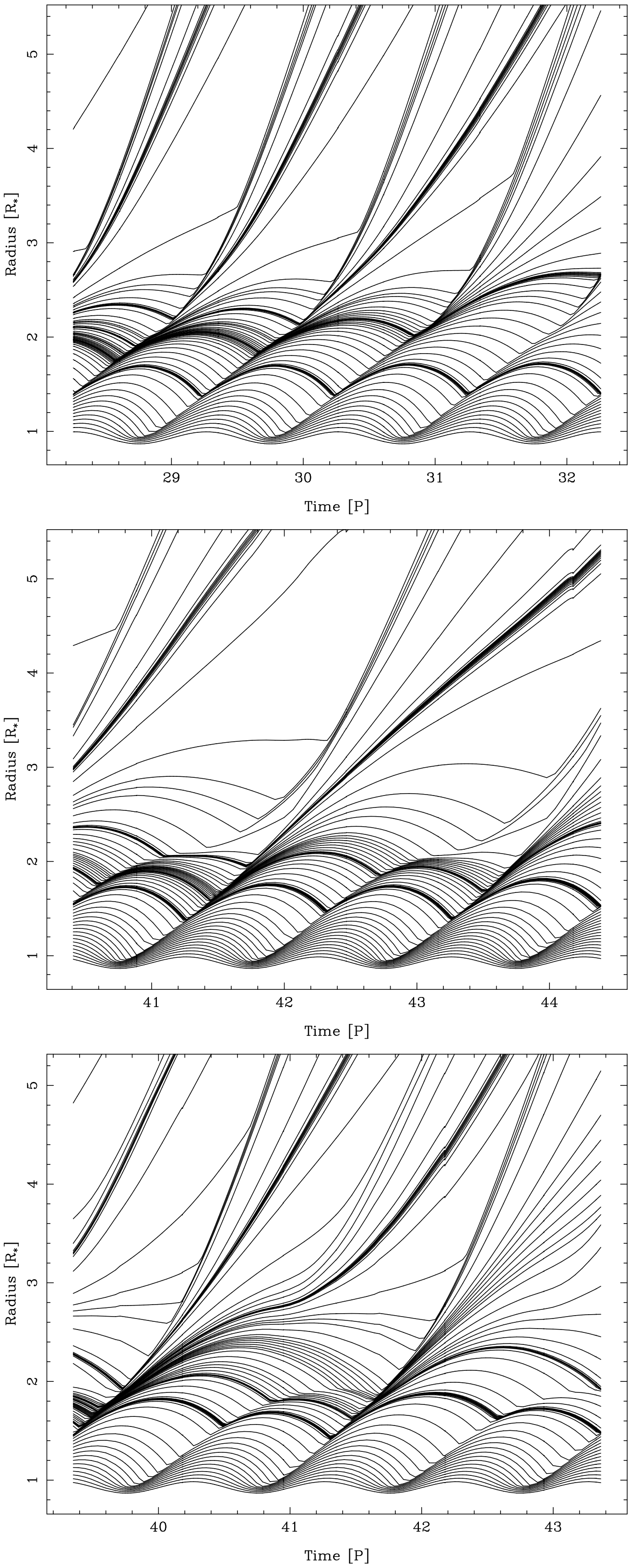

Fig. 1. Positions of selected mass shells as a function of time for models P1 (top), P2 (center) and P4 (bottom) (time in piston periods P, radius in units of the stellar radius $R_\star$ of the corresponding hydrostatic initial model).

dust tends to dominate the dynamics and thermodynamics of the circumstellar envelope.

However, most of the models presented in the literature (e.g. Fleischer et al. 1992, Winters et al. 1994, Höfner et al. 1996) are single- or multi-periodic, i.e. the dust formation and dynamics of the circumstellar envelope repeat on a timescale that is an integer multiple of the piston period P. This gives a somewhat distorted view of the situation because usually careful fine-tuning of parameters is necessary to produce such well-behaved models.

In this paper we present two groups of models (cf. Tab. 1): The parameters of series P have been chosen to produce certain periodic models which are regarded as prototypes for the following discussion. The purpose of model series R is to demonstrate the dependence of outflow characteristics (mass loss rate, terminal velocity) on various parameters. For the investigation of mass loss (cf. Sect. 4) the occurence of periodicity in some models will only be regarded as a by-product but in this section we want to demonstrate that different kinds of (multi-) periodicity can give valuable hints on the nature of the corresponding model. Since the dust formation process influences not only the dynamics but also the near IR light curves (e.g. Winters et al. 1994) detailed observations could possibly help to constrain model parameters.

3.1. Prototype models

Model P1 is a typical single-periodic model. A new dust layer is formed each piston cycle triggered by the enhanced density behind the shock waves caused by the pulsation. The dynamics of the atmosphere and the inner parts of the circumstellar envelope is depicted in Fig. 1 (top) showing the positions of selected mass shells (test particles) as a function of time. Below about 2 $R_\star$ we see the dust-free atmosphere which is periodically passed by strong shocks (marked by the sharp bends in the lines). Between 2 and 3 $R_\star$ the formation of dust layers and their subsequent acceleration due to radiation pressure (indicated by the steepening of the lines) takes place. Above, we see the innermost parts of the circumstellar dust shell and stellar wind zone (note that the distribution of the lines has no physical meaning in itself but results from the fact that the selected mass shells correspond to actual grid points in one model of the time sequence which are concentrated at shock fronts and other important spatial features).

The time-scales of the grain formation and growth depend strongly on the densities of the relevant chemical species. Therefore, if we reduce the condensible material available (by decreasing $\varepsilon_C/\varepsilon_O$) the dust formation becomes slower and the periodicity vanishes. In model P2 (which differs from model P1 by a lower value of $\varepsilon_C/\varepsilon_O$) we encounter a simple form of multiperiodicity: A dust layer is formed every second piston period (Fig. 1, center).

A different kind of multiperiodicity is observed in model P4 (model V1 in Höfner et al. 1996). A dust layer is formed every piston period but alternately this process is triggered by a passing shock (as in the single-periodic model P1) or occurs spontaneously (i.e. without a density enhancement caused by a shock) in the wake of the preceeding dust shell, above the next dust-free shock wave created by the pulsation (Fig. 1, bottom). In Höfner et al. (1996) we have interpreted this behaviour as a consequence of a higher background density of the atmosphere compared to a single-periodic model. The mass loss rate (which can be used as an indicator of the density in the acceleration region of the outflow) is more than a factor of two higher than in the single-periodic model P1. Actually, the effective temperature of model P4 is 100 K cooler than in model P1 which – for a given luminosity – leads to a more extended stellar atmosphere.

A similar effect can be achieved by changing the luminosity while keeping the effective temperature constant. The luminosity of model P3 is about 15 percent higher than in model P1 and the carbon abundance is the same as in the cooler model P4. Note, that the stellar radii of models P3 and P4 are almost identical. P3 and P4 show a similar multiperiodic behaviour and the mass loss rates are comparable.

3.2. A random sample

If we regard model series R (cf. Tab. 1) we find that only 2 of the 17 models show a well-defined periodicity of the circumstellar dust shell. Model R5P is single-periodic and model R10C18 shows a multiperiodic behaviour similar to models P3/P4. About half of the remaining models exhibit a quasi-periodicity (indicated by a 'q' behind the corresponding period) and the rest shows irregular temporal variations.

The relation between models R7 and R7C20 is analogous to P1 and P2 in that they differ only by the carbon abundance. In the model with the higher value of $\varepsilon_C/\varepsilon_O$ (R7) a dust shell forms every piston cycle while in R7C20 the formation of a new dust layer occurs every second piston period. Model R7M has the same parameters as model R7 except for the mass which is lower by 10 percent (leading to a more extended structure of the atmosphere) and exhibits a behaviour similar to models P3/P4, i.e. a formation of dust layers once per piston period which alternately is triggered by a shock or happens spontaneously. The mass loss rate of R7M is twice as high as in model R7 supporting our argument about the mean density and this type of multiperiodicity. Models R5 and R5P which differ only by the pulsation period demonstrate the influence of time-scales. In the model with the shorter period (R5) a dust layer forms about every second period while the longer period of model R5P allows for the occurence of dust formation once each piston cycle. Note in this context that the mass loss rates and outflow velocities of the two models are almost identical.

3.3. Influence on light curves

Observable properties of LPVs like light curves are influenced both by the pulsation of the star and the dust formation in the circumstellar envelope. The pulsation (which is believed to be due to a κ-mechanism operating in the H and first He ionisation zones) is associated with changes of the luminosity, i.e. bolometric variations. In contrast, the formation of dust

Table 1. Model parameters ($L_\star$, $M_\star$, $T_\star$, $\varepsilon_{\rm C}/\varepsilon_{\rm O}$, P, $\Delta u_{\rm p}$) and results: mass loss rate $\dot{M}$, mean velocity at the outer boundary $\langle u \rangle$, mean degree of condensation at the outer boundary $\langle f_{\rm c} \rangle$ and the corresponding dust-to-gas mass ratio ρ_d/ρ_g (see text); $P_{\rm dust}$ and $P_{\rm dyn}$ are periods (in units of the piston period P) characterizing the formation of new dust layers and the dynamics of the circumstellar envelope, respectively (a 'q' behind a number indicates a quasi-periodic behaviour). $R_\star$ is the stellar radius calculated from $L_\star$ and $T_\star$. The last column gives the plot symbols used in Figs. 4 and 5.

model	$L_\star$ [$L_\odot$]	$M_\star$ [$M_\odot$]	$T_\star$ [K]	$R_\star$ [$R_\odot$]	$\varepsilon_{\rm C}/\varepsilon_{\rm O}$	P [d]	$\Delta u_{\rm p}$ [km/s]	$\dot{M}$ [$M_\odot$ yr^{-1}]	$\langle u \rangle$ [km/s]	$\langle f_{\rm c} \rangle$	ρ_d/ρ_g [10^{-3}]	$P_{\rm dust}$ [P]	$P_{\rm dyn}$ [P]	symbol
P1	10000	1.0	2700	457	1.77	650	2.0	$1.0 \cdot 10^{-5}$	25	0.78	3.4	1	1	△
P2	10000	1.0	2700	457	1.49	650	2.0	$9.4 \cdot 10^{-6}$	16	0.69	1.9	2	2	△
P3	11550	1.0	2700	491	1.70	650	2.0	$2.3 \cdot 10^{-5}$	24	0.77	3.1	1	2	△
P4*	10000	1.0	2600	493	1.70	650	2.0	$2.6 \cdot 10^{-5}$	22	0.77	3.1	1	2	△
P5**	10000	1.0	2745	442	1.80	650	2.0	$1.0 \cdot 10^{-5}$	25	0.79	3.6	1	1	△
R5	5000	1.0	2970	267	2.50	295	2.0	$5.1 \cdot 10^{-7}$	28	0.55	4.7	2q	2q	○
R5C	5000	1.0	2970	267	2.30	295	2.0	$4.6 \cdot 10^{-7}$	25	0.53	3.9	2q	-	○
R5P	5000	1.0	2970	267	2.50	390	2.0	$5.6 \cdot 10^{-7}$	29	0.69	5.9	1	1	○
R7	7000	1.0	2880	336	2.50	390	2.0	$3.2 \cdot 10^{-6}$	33	0.69	5.9	1q	1q	○
R7C20	7000	1.0	2880	336	2.00	390	2.0	$1.9 \cdot 10^{-6}$	21	0.55	3.1	2q	2q	○
R7C18	7000	1.0	2880	336	1.80	390	2.0	$5.8 \cdot 10^{-7}$	7	0.37	1.7	-	-	○
R7U	7000	1.0	2880	336	2.50	390	4.0	$8.0 \cdot 10^{-6}$	34	0.72	6.1	-	-	□
R7M	7000	0.9	2880	336	2.50	390	2.0	$6.4 \cdot 10^{-6}$	32	0.62	5.3	1q	2q	□
R7C20P	7000	1.0	2880	336	2.00	525	2.0	$2.4 \cdot 10^{-6}$	19	0.52	2.9	-	-	○
R10	10000	1.0	2790	428	2.00	525	2.0	$1.1 \cdot 10^{-5}$	27	0.65	3.7	1q	2q	○
R10C18	10000	1.0	2790	428	1.80	525	2.0	$1.6 \cdot 10^{-5}$	25	0.71	3.2	1	2	○
R10C16	10000	1.0	2790	428	1.60	525	2.0	$9.3 \cdot 10^{-6}$	19	0.71	2.4	2q	-	○
R10C15	10000	1.0	2790	428	1.50	525	2.0	$2.8 \cdot 10^{-6}$	5	0.43	1.2	-	-	○
R13	13000	1.0	2700	521	1.40	650	2.0	$5.9 \cdot 10^{-6}$	7	0.45	1.0	-	-	○
R13C16	13000	1.0	2700	521	1.60	650	2.0	$2.9 \cdot 10^{-5}$	21	0.72	2.4	-	-	○
R13U	13000	1.0	2700	521	1.40	650	6.0	$4.5 \cdot 10^{-5}$	13	0.60	1.4	-	-	□
R13MU	13000	0.9	2700	521	1.40	650	6.0	$8.3 \cdot 10^{-5}$	15	0.69	1.6	-	-	□

* equal to model V1 in Höfner et al. (1996) ** equal to model V2 in Höfner et al. (1996)

layers basically causes a spectral redistribution of the stellar radiation. The grains absorb effectively at short wavelengths and reemit the energy at longer wavelengths. Thus, in principle, it should be possible to disentangle the variability caused by stellar pulsation from the effects of dust formation and dynamics in the atmosphere by a simultaneous photometric monitoring of LPVs at different wavelengths. A possible (multi-) periodicity in combination with known outflow characteristics (velocity, mass loss rate) could then help to restrict model parameters like e.g. the abundance of the condensible material.

Winters et al. (1994) have calculated light curves of C-stars based on dynamical models of the circumstellar dust shell which are – regarding the physical input – largely comparable to the models presented here (cf. Höfner et al. 1996 for a discussion). They demonstrate that the formation of dust layers decisively influences the shape of the light curves and that the dynamics of the circumstellar dust shell (e.g. multiperiodicity) may be reflected in the long-term behaviour, i.e. variations of the light curve over several pulsation periods which are superimposed on the variation caused by the pulsation. Note that such features are actually found in observed light curves of LPVs (e.g. Le Bertre 1992). Preliminary calculations of near-IR light curves based on our own models seem to support the results of Winters et al. (1994). In the case of the multiperiodic model P4 we find – depending on the wavelength and thus on the spatial region where the radiation comes from – a periodicity of the light curves on a time-scale of either 1 or 2 P.

4. Mass loss

In contrast to the preceeding section we now are interested in time-averaged quantities characterizing the mass loss, i.e. the mass loss rates and the outflow velocities of the models. We

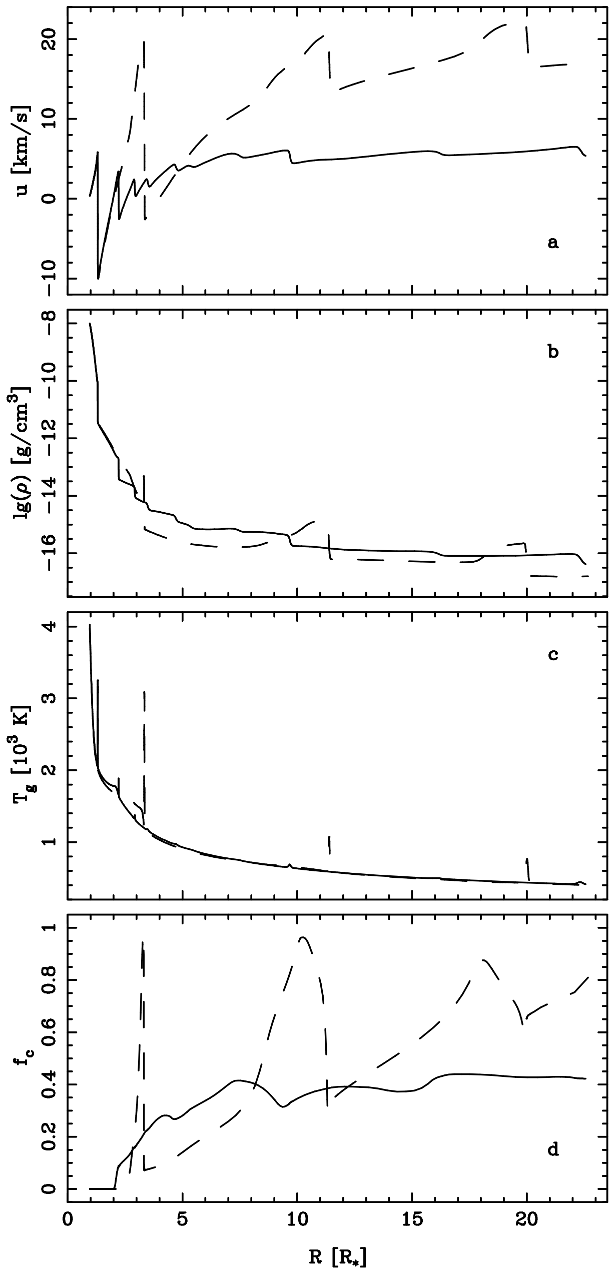

Fig. 2. Radial structure of models R10C16 (dashed) and R10C15 (full line): velocity (a), density (b), gas temperature (c) and degree of condensation (d).

investigate their dependence on various physical parameters and compare the modelling results to observations.

4.1. Parameter dependence

According to their influence on the models, the physical parameters can be split into the following groups: $L_\star$, $M_\star$ and $T_\star$ determine the spatial structure of the hydrostatic initial model and, consequently, (to a certain extent) the background structure of the inner parts of the dynamical model. P and $\Delta u_{\rm p}$ characterize the stellar pulsation (period and amplitude) and thus the levitation of the atmosphere. Together these parameters largely determine the conditions in the dust condensation zone while $\varepsilon_{\rm C}/\varepsilon_{\rm O}$ controls the efficiency of grain formation and growth for given temperature and density.

Models R7, R7C20 and R7C18 show the effects of different carbon abundances while all other parameters are held constant. Comparing the differences of $\dot{M}$ and $\langle u\rangle$ between the models R7 and R7C20 as well as R7C20 and R7C18, the larger change in the abundance of condensible carbon $\tilde{\varepsilon}_{\rm C} = (\varepsilon_{\rm C}/\varepsilon_{\rm O} - 1)\,\varepsilon_{\rm O}$ in the first pair causes only a relatively small effect compared to the second pair. This nicely demonstrates the non-linearities of the dust condensation and wind mechanism. As long as the models are in a parameter domain where both the dust condensation and radiative driving work efficiently, $\dot{M}$ depends only slightly on $\tilde{\varepsilon}_{\rm C}$. However, as the abundance of condensible carbon is reduced it becomes more and more difficult to drive a stellar wind and $\dot{M}$ starts to decline significantly with decreasing $\tilde{\varepsilon}_{\rm C}$. The same effect is seen in models R10, R10C18, R10C16 and R10C15, another series of models with different values of $\varepsilon_{\rm C}/\varepsilon_{\rm O}$ but otherwise identical parameters. Figure 2 shows models R10C16 and R10C15 which differ less than 20 percent in $\tilde{\varepsilon}_{\rm C}$ but exhibit a completely different spatial structure. R10C16 shows a pronounced shell-like structure associated with strong shock waves and complete condensation occuring within the dust layers. R10C15 exhibits only small variations in the various quantities plotted, the maximum degree of condensation is far from complete and both the velocity and the mass loss rate are significantly lower than in model R10C16.

A moderate change of the pulsation period seems to have little effect on the mass loss rate and the velocity as inferred from models R5 and R5P or models R7C20 and R7C20P, respectively. The piston velocity amplitude on the other hand may have considerable influence on the mass loss as demonstrated by models R7 and R7U as well as models R13 and R13U. The mass loss rate increases with $\Delta u_{\rm p}$ since (for given stellar parameters) the shock waves caused by the pulsation determine the density in the dust condensation and wind acceleration region and thus $\dot{M}$.

Models R5 and R7, R7C20 and R10 as well as R10C16 and R13C16 show how a combined change of $L_\star$ and $T_\star$ due to an evolution along the AGB (with $M_\star$, $\varepsilon_{\rm C}/\varepsilon_{\rm O}$ and $\Delta u_{\rm p}$ held constant and $P(L_\star)$ changing accordingly) affects the mass loss. Since both increasing $L_\star$ and decreasing $T_\star$ lead to more extended atmospheres, the mass loss rate increases strongly. As the mass loss at the same time reduces $M_\star$ the effect will even be larger. A comparison of models R7 and R7M or models R13U and R13MU demonstrates how sensitively the mass loss depends on $M_\star$.

For stellar winds which are driven by radiation pressure on dust a close correlation should exist between the outflow velocity and the strength of radiation pressure relative to gravitation. In Fig. 3 we have plotted $\langle u\rangle$ as a function of the quantity

$$\hat{\alpha} = \left(\frac{\rho_d}{\rho_g}\right)\,\frac{L_\star}{M_\star} \propto \left(\frac{4\pi}{c}\,\kappa_{\rm d}\,\rho\,H\right)\,\left(\frac{r^2}{G\,m_{\rm r}\,\rho}\right) \qquad (1)$$

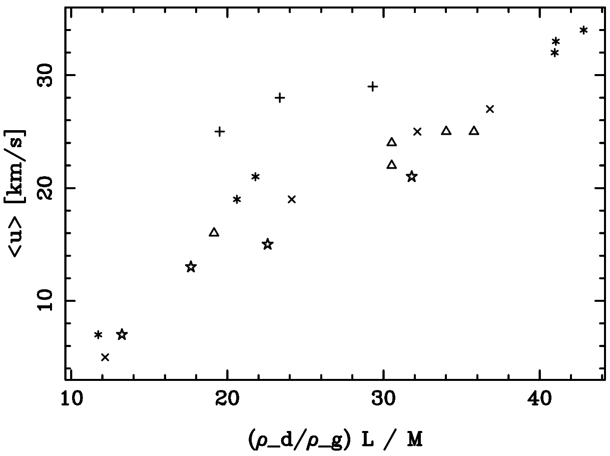

Fig. 3. Outflow velocity as a function of a quantity characterizing the strength of radiation pressure relative to gravitation; symbols for models of series R: $L_\star = 5000\,L_\odot$ (+), $L_\star = 7000\,L_\odot$ ($*$), $L_\star = 10000\,L_\odot$ ($\times$), $L_\star = 13000\,L_\odot$ ($\star$); models of series P are represented by triangles.

which is proportional to the ratio of the radiation pressure term and the gravitation term in the equation of motion. The dust opacity $\kappa_{\rm d}$ is proportional to the dust-to-gas mass ratio ρ_d/ρ_g which is related to the degree of condensation $f_{\rm c}$ by

$$\frac{\rho_d}{\rho_g} = \frac{m_{\rm C}}{m_{\rm H} + m_{\rm He}\,\varepsilon_{\rm He}}\,\tilde{\varepsilon}_{\rm C}\,f_{\rm c} = \frac{12}{1.4}\,(\varepsilon_{\rm C}/\varepsilon_{\rm O} - 1)\,\varepsilon_{\rm O}\,f_{\rm c} \qquad (2)$$

where $m_{\rm C}$, $m_{\rm H}$ and $m_{\rm He}$ are the atomic masses of carbon, hydrogen and helium and $\varepsilon_{\rm He}$ is the helium abundance. ($\varepsilon_{\rm He} = 0.1$, $m_{\rm C}/m_{\rm H} = 12$, $m_{\rm He}/m_{\rm H} = 4$; $\log(\varepsilon_{\rm O}) = -3.18$). We find a good correlation of $\langle u\rangle$ and $\hat{\alpha}$ except for the models of series R5 which lie distinctly above the bulk of the models. We interpret this as a consequence of a larger relative importance of the momentum input by the piston in the models with lower luminosities.

Note that in our sample of models no apparent correlation exists between the outflow velocity and the mass loss rate. Depending on the stellar parameters and pulsational properties a wide range of combinations seems possible.

4.2. Comparison with observations

In Fig. 4 we have plotted the mass loss rate versus the pulsation period to compare the modelling results with mean $\dot{M}$–P relations deduced from observations of Miras. We find good agreement with the results of Groenewegen (1995, for carbon Miras) and Whitelock (1990, O-rich Miras in the Galactic Bulge), especially when considering the fact that the scatter in each of the observed relations is about 1 dex for a given period and that a certain overlap exists between C- and O-rich objects. Note that the range of possible mass loss rates for a given period can be can be accounted for by differences of the pulsation amplitude (e.g. models R13 and R13U, P = 650 d) or the abundance of condensible material (non-linearities in the dust formation and radiative acceleration process; e.g. model series R10, P = 525 d).

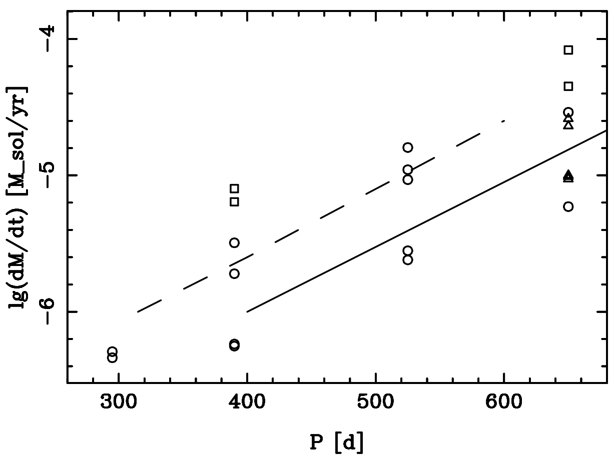

Fig. 4. Comparison of modelling results with mean $\dot{M}$–P relations deduced from observations: Groenewegen (1995, for carbon Miras; full line), Whitelock (1990, O-rich Miras in the Galactic Bulge; dashed line). Note that the scatter in the observed relations is about 1 dex for a given period.

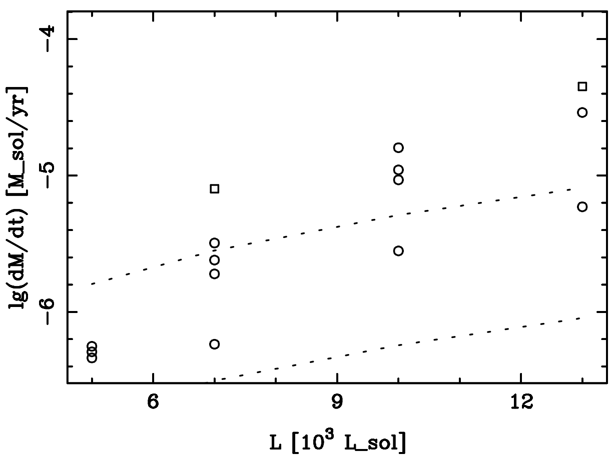

Fig. 5. Comparison of modelling results (only models of series R with $M_\star = 1 M_\odot$ are plotted) with the mass loss law of Reimers (1975) for $\eta = 1/3$ and $\eta = 3$ and corresponding stellar parameters (dotted lines).

The periods of model series R have been chosen according to the rather well established P–L relation for O-rich Mira variables (e.g. Feast et al. 1989, Whitelock 1993). In general, the periods of C-rich Miras are expected to be somewhat longer at a given luminosity than for their O-rich counterparts. However, as demonstrated in the preceeding section the mass loss rate does not depend critically on P. Using larger values of P for a given model would then basically result in shifting the points plotted in Fig. 4 to the right (higher periods) as inferred from models R5/R5P and R7C20/R7C20P. Recently, Groenewegen & Whitelock (1996) have derived a revised P–L relation ($M_{bol} = -2.59 \log P + 2.02$) for carbon Miras in the Galaxy. Interpolating for the corresponding periods between models R5 and R5P ($L_\star = 5000\,L_\odot \rightarrow 334$ d) or R7C20 and R7C20P ($L_\star = 7000\,L_\odot \rightarrow 463$ d) leads to points that coincide with the mean $\dot{M}$–P relation for carbon Miras of Groenewegen (1995).

In Fig. 5 we compare our results to the well-known mass loss law of Reimers (1975)

$$\dot{M} = 4 \cdot 10^{-13}\,\eta\,\frac{L_\star\,R_\star}{M_\star} \qquad [\mathrm{M}_\odot\ \mathrm{yr}^{-1}] \tag{3}$$

($L_\star$, $R_\star$ and $M_\star$ in solar units) which – directly or with modifications – has been widely used in calculations of AGB evolution though it was originally found for RGB stars. While at $L_\star = 5000\,L_\odot$ the models lie within the range defined by the parameter η the mass loss in our models increases much steeper with luminosity so that at $L_\star = 13000\,L_\odot$ there is practically no overlap with the range given by Reimers' law. Recent evolution calculations by Blöcker (1995) use different mass loss laws for the RGB, AGB and post-AGB phases. During the AGB phase mass loss is described by a modified version of Reimers' law based on the dynamical models of Bowen (1988). An additional factor depending on $L_\star^{2.7}$ leads to a steeper increase of mass loss with luminosity (about one order of magnitude for the range plotted in Fig. 5) which is in much better agreement with the results presented here.

5. Conclusions

To investigate the atmospheric dynamics and mass loss of C-rich long-period variables we have calculated radiation-hydrodynamical models of the atmosphere and circumstellar dust shell which include a detailed description of the dust condensation. Simulating the stellar pulsation by a variable inner boundary we have varied the physical parameters of the models systematically to demonstrate their influence on the time-dependent behaviour and time-averaged mass loss characteristics of our models.

The dependence of the mass loss rate on stellar parameters predicts a strong increase of mass loss as stars evolve along the AGB. As the stellar luminosity increases, while simultaneously the mass and effective temperature decrease, the atmosphere becomes more extended which leads to more favourable conditions for dust formation and higher densities in the acceleration region of the wind. In accordance with Bowen & Willson (1991) we argue that the development of a "superwind" ($\dot{M} \sim 10^{-5} - 10^{-4}\,\mathrm{M}_\odot\ \mathrm{yr}^{-1}$) is a natural consequence of the evolution of stellar parameters on the AGB. The increase of mass loss with luminosity in our models is much steeper than predicted by Reimers' law (which was found empirically for the RGB, not the AGB) and is in reasonable agreement with the description of mass loss used by Blöcker (1995) for calculating stellar evolution on the AGB.

The models presented in this paper agree nicely with mean mass loss–period relations deduced from observations (Groenewegen 1995, Whitelock 1990). The observed scatter of mass loss rates for a given period (about one order of magnitude) can be reproduced with the models, e.g. by differences in the pulsation amplitude (which affects the shock strength and, consequently, the levitation of the atmosphere) or in the abundance of condensible material (non-linearities of the wind mechanism) for otherwise identical models. The wind velocities are well correlated with $\hat{\alpha} = (\rho_d/\rho_g)\,L_\star/M_\star$, a quantity characterizing the strength of radiation pressure on dust relative to gravitation.

The shape and long-term behaviour of IR light curves are determined both by stellar pulsation and dust formation. While the first leads to bolometric variations the second causes rather a spectral redistribution of the stellar radiation. Thus, in principle, it should be possible to disentangle the effects of pulsation from the physical processes in the circumstellar envelope by simultaneously monitoring LPVs in different wavelengths, probing different regions of the atmosphere and circumstellar dust shell. Since the time-dependent behaviour of the circumstellar envelope depends strongly on various model parameters this could help to restrict physical parameters of individual stars.

Acknowledgements. This work is supported by the Österr. Fonds zur Förderung der wissenschaftl. Forschung (FWF) under project number S7305–AST. We thank M. Feuchtinger, J. Hron, F. Kerschbaum, M. Schultheis and G. Wuchterl for many discussions concerning various theoretical and observational aspects of the paper.

References

Blöcker T. 1995, A&A 297, 727
Bowen G.H. 1988, ApJ 329, 299
Bowen G.H., Willson L.A. 1991, ApJ 375, L53
Dorfi E.A., Feuchtinger M. 1995, Comp. Phys. Comm. 89, 69
Feast M.W., Glass I.S., Whitelock P.A., Catchpole R.M. 1989, MNRAS 241, 375
Fleischer A.J., Gauger A., Sedlmayr E. 1992, A&A 266, 321
Fleischer A.J., Gauger A., Sedlmayr E. 1995, A&A 297, 543
Groenewegen M. 1995, Ap&SS 224, 321
Groenewegen M.A.T., Whitelock, P.A. 1996, MNRAS, in press
Habing H.J. 1996, A&AR 7, 97
Höfner S., Feuchtinger M., Dorfi E.A. 1995, A&A 297, 815
Höfner S., Fleischer A.J., Gauger A., Feuchtinger M.U., Dorfi E.A., Winters J.M., Sedlmayr E. 1996, A&A, in press
Iben I. 1984, ApJ 277, 333
Le Bertre T. 1992, A&AS 94, 377
Maron N. 1990, Ap&SS 172, 21
Reimers D. 1975, in *Problems in Stellar Atmospheres and Envelopes*, B. Baschek, W.H. Kegel, A.G. Trawing (eds.), Springer, Berlin
Whitelock P. 1993, in *Galactic Bulges,* IAU Symp. 153, eds. H. Dejonghe and H.J. Habing, Kluwer, Dordrecht, p.39
Whitelock P. 1990, PASP 11, 365
Winters J.M., Fleischer A.J., Gauger A., Sedlmayr E. 1994, A&A 290, 623
Winters J.M., Fleischer A.J., Gauger A., Sedlmayr E. 1995, A&A 302, 483
Wood R.P. 1979, ApJ 227, 220

This article was processed by the author using Springer-Verlag LaTeX A&A style file *L-AA* version 3.